DOI:10.16555/j.1006-8775.2015.02.008

Article ID: 1006-8775(2015) 02-0171-14

IMPROVEMENT OF OCEAN DATA ASSIMILATION SYSTEM AND CLIMATE PREDICTION BY ASSIMILATING ARGO DATA

LI Qing-quan (李清泉)[1, 2], ZHANG Ren-he (张人禾)[3], LIU Yi-min (刘益民)[3]

(1. Laboratory for Climate Studies, National Climate Center, China Meteorological Administration, Beijing 100081 China; 2. Collaborative Innovation Center on Forecast and Evaluation of Meteorological Disasters , Nanjing University of Information Science & Technology, Nanjing 210044 China; 3. State Key Laboratory of Severe Weather, Chinese Academy of Meteorological Sciences, Beijing 100081 China)

Abstract: The Argo (Array for Real-time Geostrophic Oceanography) data from 1998 to 2003 were used in the Beijing Climate Center-Global Ocean Data Assimilation System (BCC-GODAS). The results show that the utilization of Argo global ocean data in BCC-GODAS brings about remarkable improvements in assimilation effects. The assimilated sea surface temperature (SST) of BCC-GODAS can well represent the climatological states of observational data. Comparison experiments based on a global coupled atmosphere-ocean general circulation model (AOCGM) were conducted for exploring the roles of ocean data assimilation system with or without Argo data in improving the climate predictability of rainfall in boreal summer. Firstly, the global ocean data assimilation system BCC-GODAS was used to obtain ocean assimilation data under the conditions with or without Argo data. Then, the global coupled atmosphere-ocean general circulation model (AOCGM) was utilized to do hindcast experiments with the two sets of the assimilation data as initial oceanic fields. The simulated results demonstrate that the seasonal predictability of rainfall in boreal summer, particularly in China, increases greatly when initial oceanic conditions with Argo data are utilized. The distribution of summer rainfall in China hindcast by the AOGCM under the condition when Argo data are used is more in accordance with observation than that when no Agro data are used. The area of positive correlation between hindcast and observation enlarges and the hindcast skill of rainfall over China in summer improves significantly when Argo data are used.

Key words: Argo data; ocean data assimilation; climate prediction; AOGCM

CLC number: P731.11 **Document code:** A

1 INTRODUCTION

In recent years, extreme climate events occurred frequently as the global climate was getting warm, which brought significant influences to national economy and social development. Short-term climate prediction is an emphasis of the international climate research program "Climate Variability and Predictability" (WCRP)[1]. In recent years, as coupled numerical models for short-term climate prediction are continually developed and refined, more and more attention has been paid by scientists in various countries to the negative impacts of the errors in initial conditions for models (especially, the errors of initial oceanic conditions) on the prediction results of models. Short-term climate prediction depends greatly upon oceanic observational data, such as temperature, salinity, currents, etc. As a key member of climate system, the ocean plays important roles on climate anomalies. Climate anomalies of China are closely related with the variation of ocean heat conditions. Existing research results indicate that sea temperature anomalies will influence the climate of China (Li et al.[2-3]; Rong et al.[4]). Because oceanic observational data are insufficient, coupled models cannot behave perfectly and the accuracy of climate prediction cannot be satisfactory. The aim of the oceanic data assimilation is to provide the initial signals of the most important anomalous oceanic condition for the model system of short-term climate prediction so as to improve the accuracy of numerical climate prediction (Zheng et al.[5-8]).

The Argo (Array for Real-Time Geostrophic Oceanography) observation plan was originally brought forward by atmospheric and oceanic scientists of the United States and Japan in 1998. It gains worldwide concern and support rapidly. In 2000, an international Argo program came into formal effect. It is a sub-program of the Global Oceanic Observation System (GOOS) and gains great support from the Climate Variability and Predictability (CLIVAR), which is affiliated to the World Climate Research Program (WCRP), as well as

Received 2014-06-19; **Revised** 2015-02-09; **Accepted** 2015-04-15

Foundation item: National Program on Key Basic Research Project of China (2012CB955203,2013CB430202); National Natural Science Foundation of China (40231014,41175065); China Meteorological Administration R&D Special Fund for Public Welfare (meteorology) (GYHY201306021); National High Technology Research and Development Program of China (2010AA012404)

Biography: LI Qing-quan, Ph.D., research fellow, primarily undertaking research on climatic diagnosis and numerical simulation.

Corresponding author: LI Qing-quan, e-mail: liqq@cma.gov.cn

the Global Oc eanic Data Assimilation Experiments (GODAE). China formally joined in the international Argo program in October 2001. Up to January 2014, 19 countries have placed approximately 4 000 Argo profile floats in the Pacific, Indian, and Atlantic Oceans. By far, although some floats have stopped working due to technical or communication faults, 2 483 floats still work normally (China Argo Real-time Data Center[9]). Each float sends a set of profile data of the upper 2 000-m oceanic temperature and salinity every 10 days. The floats are placed in the ocean at roughly every 3° longitudes by 3° latitudes. The datasets are rapidly transmitted to climate or oceanic prediction centers through the Global Telecommunications System (GTS) and used for routine operations. The transmission time is normally shorter than 24 h. Therefore, the Argo program can provide observational temperature, salinity, and current data of wide-range, real-time, multi-layer, and high spatio-temporal resolution in more than 100 000 profiles of the upper oceans each year. All Argo data are open to public without ownership limit. The implement of this program will make an unprecedented and long-term tracking observation on seasonal and decadal variation of oceans, and thus provide a dataset of global subsurface ocean and lead to great advance in the understanding and prediction of climate.

Argo data provide a unique opportunity for the improvement of the initial condition of ocean models and the skill of short-term climate prediction. At present, the US National Environmental Prediction Center (NCEP), British Hadley Climate Center, and Australian Bureau of Meteorological Research Center (BMRC) have introduced Argo assimilation data into experimental and operational prediction (Xu[10]). Various active researches on the application of Argo data are now underway. For example, Xu et al.[11] and Liu et al.[12] have studied the relationship between tropical cyclones and the Northwest Pacific. Pan and Liu [13] studied the impact of mesoscale eddies on vertical mixture in the North Pacific. Zhang et al.[14] improved the tropical oceanic modeling of intermediate complexity by using Argo data. Liu et al.[15] introduced Argo data into the Beijing Climate Center-Global Ocean Data Assimilation System (BCC-GODAS) to well reproduce the observational patterns, seasonal variability, and anomalous characteristics of sea temperature (Zhang and Li[16]).

The present paper is a continued study after Argo data was introduced in BCC-GODAS. Section 2 shows the assimilation results of BCC-GODAS with Argo data used. In section 3, the oceanic assimilation data are adopted in a global atmosphere-ocean coupled model. Through historical hindcast experiments, the impacts of Argo assimilation data on the seasonal prediction of the coupled model are analyzed and discussed. Finally, conclusions and discussions are given in section 4.

2 APPLICATION OF ARGO DATA IN BCC–GODAS

BCC-GODAS is a part of the operational climate model prediction system in Beijing Climate Center (Liu et al.[17]). It comprises four sub-systems: 1) data pre-processing sub-system, mainly used for data collection, decoding, quality control, and standardization; 2) real-time wind stress calculating sub-system, in which real-time sea surface observational data are used to compute wind stress, and analyzed fields on global model grids are obtained by using an optimal interpolation method; 3) variational analysis and interpolation sub-system, in which 3-dimensional space variation and a time window of 4-week width is employed, and observational data are interpolated according to certain weights; 4) dynamical oceanic model sub-system. The oceanic model is the L30T63 OGCM (Jin et al.[18]), used as a global ocean circulation model in the operational prediction system.

The observation data used in BCC-GODAS are air temperature, air pressure and wind at the sea surface, as well as ocean temperature, etc. These data are mainly derived from the GTS datasets and the historical datasets from the Information Center of China Meteorological Administration (CMA). BCC-GODAS can well reflect the variation of the tropical Pacific sea surface temperature (SST) (Liu et al.[15]). However, it still has some deficiencies. The anomalies of the equatorial western Pacific SST and sub-surface temperature of BCC-GODAS are not intensive enough. In the middle latitudes, the correlation between assimilated and observed temperature anomalies is low. The major reasons are due to data amount, error matrix, dynamic model, etc. In order to improve the results of oceanic data assimilation, Liu et al. [15] introduced Argo data into the BCC-GODAS assimilation system. The data are global Argo data starting from 1998, which are provided by China Argo Real-time Data Center. Considering the absolute value and gradient of the data, the Argo data are processed in primary quality control and the obviously unreasonable data are eliminated. The Argo data are interpolated into the model levels and then the data assimilation system is utilized to get the assimilation data. In this paper, the performance of BCC-GODAS is also analyzed.

In Fig.1, the SST in 1982-2003 derived from BCC-GODAS with Argo data are compared with the optimal interpolated SST (OISST) of US National Oceanic and Atmospheric Administration. It can be seen that BCC-GODAS can well capture SST condition. The distribution of the assimilated SST in the Pacific, Indian, and Atlantic Oceans are generally consistent with the observations. For example, in the tropical western Pacific warm pool and the equatorial eastern Pacific cold tongue, the features of the distribution range and pattern, and the magnitude of sea temperature agree well with observations (see Fig.1a and 1b). In the region between 30°N and 30°S, the departure between assimilated SST and OISST is generally below 0.5℃, except for the large difference (about 1.0℃) in the equatorial eastern Pacific along the South American coasts and in the Southwestern Atlantic along the southern Africa. In the middle and high latitudes of the two hemispheres, there are relatively large differences between the climate state of assimilated sea temperature and observation, which are generally above 0.5℃ (see Fig.1c). From the correlation between BCC-GODAS SST anomalies and observations (as shown in Fig.1d), it can also be seen that the correlation coefficients in low latitudes are higher than those in the middle and high latitudes. The correlation coefficients in the equatorial central and eastern Pacific is generally above 0.8, with the highest being about 0.9. In Niño3 (5°N to 5°S, 150°W to 90°W) and Niño3.4 areas (5°N to 5°S, 120°W to 170°W) of the equatorial Pacific, the averaged correlation coefficients are 0.87 and 0.90, respectively. The correlation coefficients in most areas of the three oceans between 60°N and 60°S are positive (accounting for 90.84%), where the mean value is 0.37. The globally averaged correlation coefficient is 0.30. The grid number of positive correlation accounts for 83.57%. The grid number of positive correlation reaching or exceeding the 95% confidence level (with correlation coefficients being equal to 0.42) accounts for 33.62%.

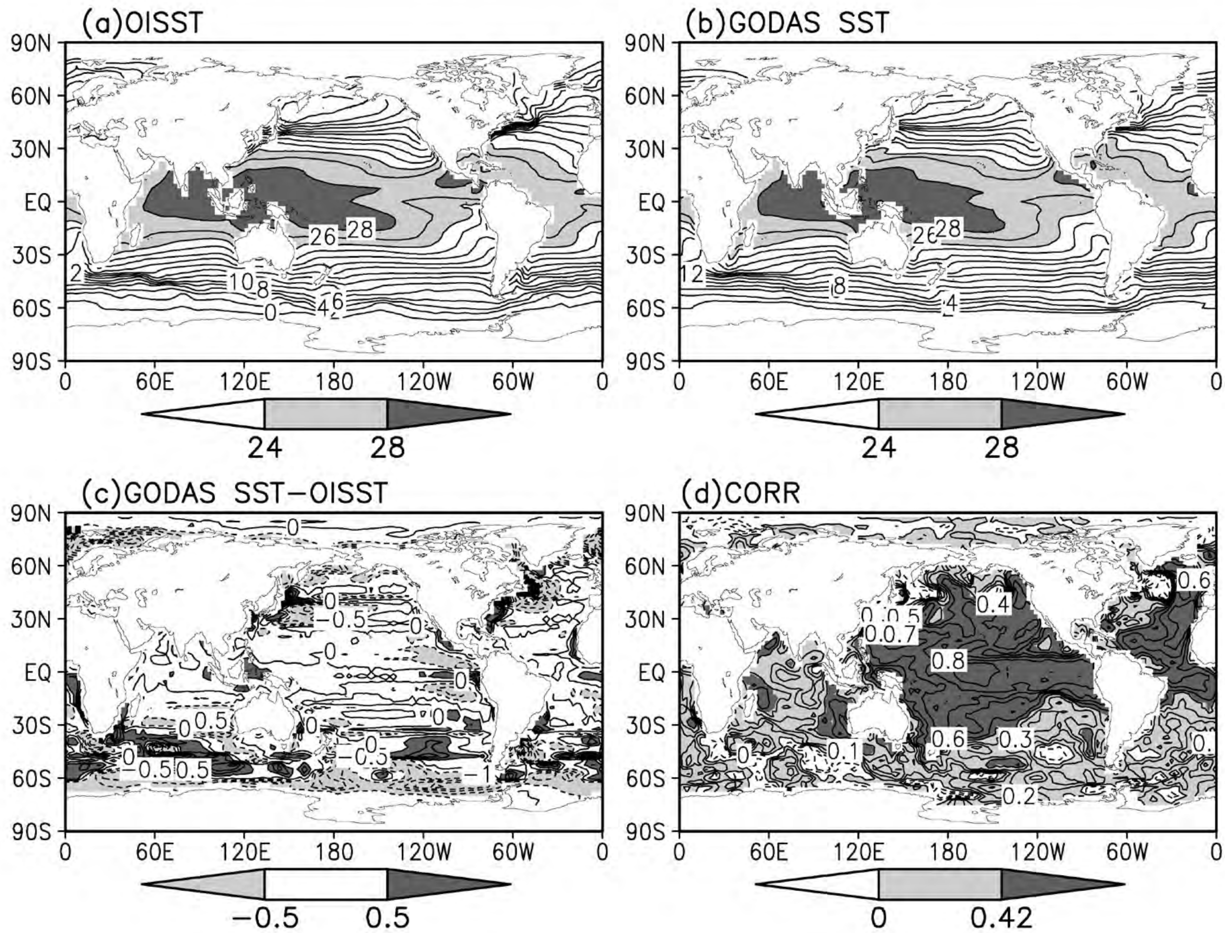

Figure 1. Comparison between BCC-GODAS SST and OISST in 1982-2003. (a) OISST; (b) BCC-GODAS SST; (c) differences between BCC-GODAS SST and OISST; (d) correlation coefficient between BCC-GODAS and OISST anomalies. Contour intervals are 2℃ in (a) and (b), and 0.5℃ in (c), respectively. Light shadings in (d) indicate positive correlation, and dark higher than 95% confidence level.

The assimilation data of BCC-GODAS from 1982 to 2003 are not only compared with observed SST, but also compared with the assimilated sea temperature data of NCEP's Global Ocean Data Assimilation System (NCEP_GODAS for short). The correlation between the two sets of assimilated SST anomalies is shown in Fig. 2. Except for negative correlation in the northern Pacific beyond 40°N and 40°S, there is positive correlation in all other regions. The grid number of positive correlation accounts for 89.17%. The mean correlation coefficients are 0.62 between 30°N and 30°S and 0.44 between 60°N and 60°S, respectively. The highest correlation occurs in the tropical Pacific between 8°N and 10°S, with correlation coefficients mostly around 0.8 and the maximum above 0.9. The mean SST anomalies are 0.85 and 0.89 respectively in the Niño3 and Niño3.4 regions. Fig.2b shows the longitude-depth distribution of correlation between BCC-GODAS and NCEP_GODAS sea temperature anomalies along equator (5°N-5°S). In the upper ocean (0 to 540 m) of the Pacific, all correlation coefficients are positive. In most areas, the correlation coefficients of sea temperature anomalies in the upper 250 meters reach the 95% confidence level. Bellow 250 meters, however, the correlation coefficients in the equatorial eastern Pacific (80°-100°W) are better than in the equatorial western Pacific (120°-140°E). The correlation between BCC-GODAS and NCEP_GODAS sea temperature anomalies below 250 meters is not as good as that above 250 meters in the Pacific. The correlation relationship is good (positive) in the Indian Ocean above 500 meters, and the correlation coefficients reach or exceed the significant level in the ocean above 100 meters and between 250 and 450 meters. There is good relationship in the Pacific above 450 meters, and the correlation coefficients reach or exceed the significance level in the ocean above 50 meters and between 200 and 400 meters. The differences between the two sets of assimilation SST might be due to the differences of models and assimilation methods, or the differences of used observation data.

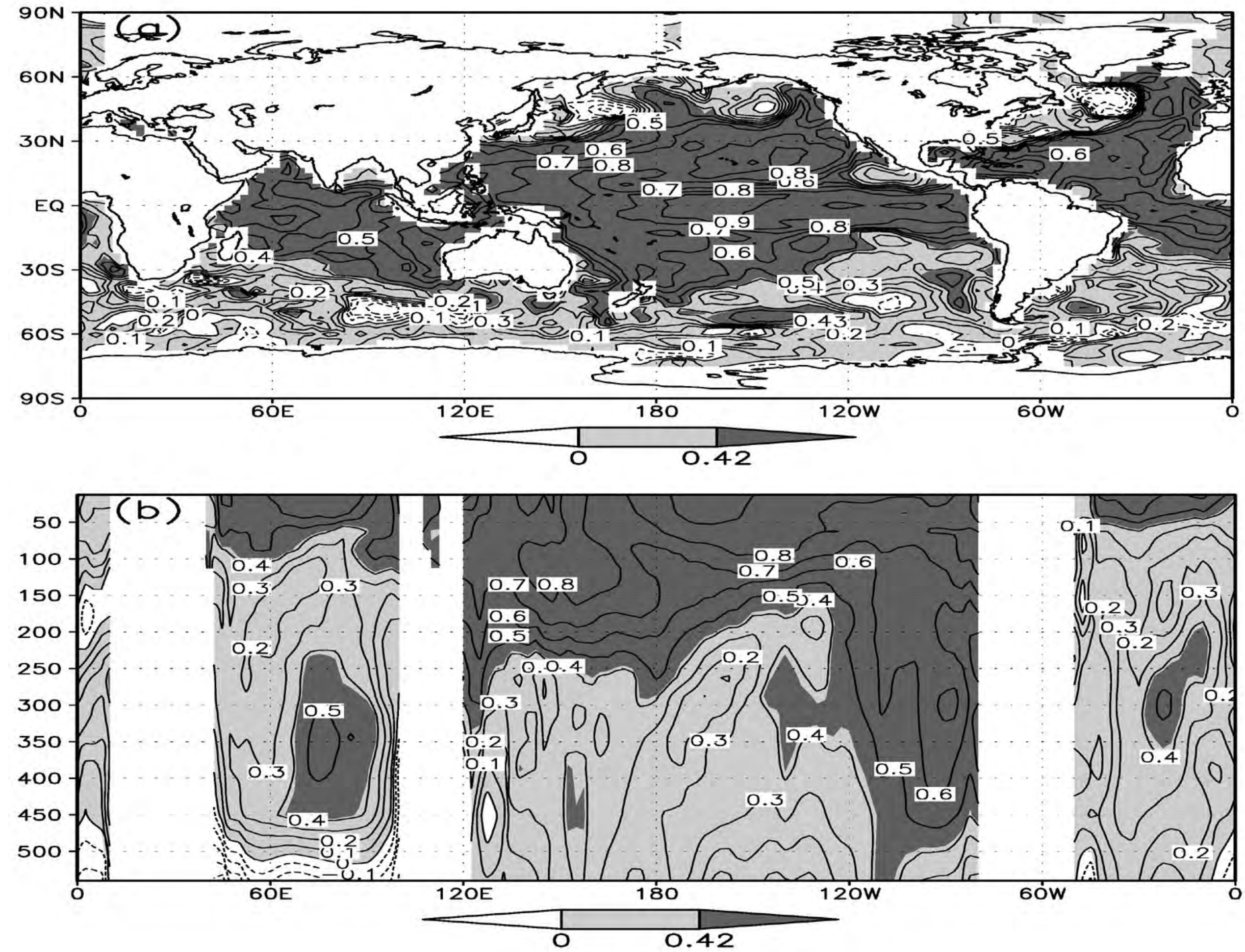

Figure 2. Correlation coefficients between BCC-GODAS and NCEP_GODAS assimilated sea temperature anomalies in 1982-2003. (a) correlation coefficients of SST anomalies; (b) correlation coefficients of sea temperature anomalies along equatorial longitude-depth section. Light shadings indicate positive correlation, and dark higher than 95% confidence level.

The above analyses are mainly based on the assimilation data of BCC-GODAS with Argo data in 1982-2003. International Argo data formally started to implement in the end of 2000, so Argo data mostly appears after 2000. Fig.3 shows the differences between the root mean squared error (RMSE) of the assimilated SST of BCC-GODAS with Argo data and OISST, and between RMSE of the assimilated SST of BCC-GODAS without Argo data and OISST during 2001-2003. From Fig.3, it can be seen, when Argo data are used, the assimilation effects of BCC-GODAS vary in different maritime space. Generally the RMSE of SST decreases in most other regions except for some areas such as areas around 45°E and 35°S (see Fig.3a). In the Atlantic, the assimilation data are obviously better to the north of the equator than to the south of it (see Fig.3b). The maximum decline of RMSE occurs in the Atlantic, followed by the Indian and Pacific Oceans (see Fig.3a), because there are some observational database originally (such as Expendable Bathythermogragh data) in the tropical Pacific, while the observation data are relatively poor in other regions (such as the Atlantic Ocean). Therefore, application of the Argo data in the assimilation system helps improve the assimilation results. In view of the regions where presently Argo floats are set, most floats are located in the Atlantic, followed by the Pacific and Indian Ocean. In the oceans to the south of 40°S, the floats are relatively spare. As the Argo observation program continues and further implements, the status of data in these areas will be improved gradually.

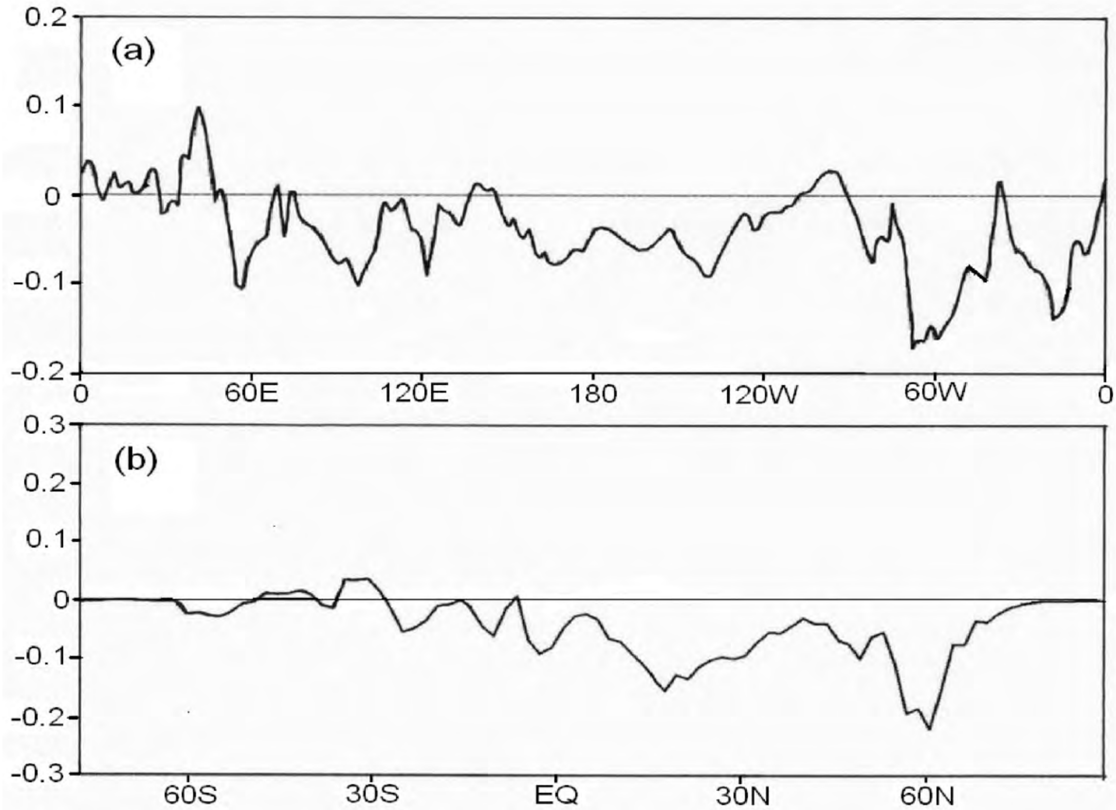

Figure 3. Differences between RMSE of BCC-GODAS SST with Argo data and OISST and RMSE of BCC-GODAS SST without Argo data and OISST during 2001-2003. (a) latitudinal average; (b) longitudinal average. Unit: ℃.

3 APPL ICATION OF ARGO DATA IN CLIMATE PREDICTION BY A GLOBAL COUPLED AOGCM

3.1 *General hindcasting performance*

It has been indicated that maritime observation data are processed with assimilation techniques and then used as initial model condition, which effectively enhance the simulation and prediction capability of numerical model (Zheng et al.[5-8]; Jia et al.[19]; Li et al.[20]; Li and Zhao[21]). Therefore, in this study, the oceanic assimilation data derived from BCC-GODAS with Argo data are used as the initial fields of a global atmospheric-oceanic coupled model in order to test the improvement of the predictive skill of the coupled model for short-term climate variability. The global coupled atmosphere-ocean general circulation model (AOGCM) used in this study is a part of the operational climate model system of BCC (Li et al.[22]). It consists of a global atmospheric circulation model (T63L16 AGCM) and a global ocean circulation model (L30T63 OGCM), which are coupled through the Daily Flux Anomaly (DFA) coupling scheme (Yu and Zhang [23]). The resolution of T63L16 AGCM is 1.875°×1.875° in the horizontal direction and 16 levels in the vertical direction. The horizontal resolution of L30T63 OGCM is 1.875°×1.875° and there are 30 levels in the vertical direction (Jin et al.[18]). The OGCM is the same as the ocean model used in BCC-GODAS. The L30T63 OGCM can simulate the climatological state of oceanic temperature, salinity, and current reasonably (Jin et al.[18]), but it does not resolve the equatorial Kelvin waves well, which may cause the simulated variation of sea temperature on the interannual time scale to depart from the observation. For example, Yu et al. [24] used the reanalysis wind stress data from 1979 to 1993 and climatological mean heat flux to force the L30T63 model and a high-resolution oceanic model LICOM, respectively. The horizontal resolution of LICOM is 0.5°×0.5° and its vertical resolution is 30 levels (Liu et al.[25]). The results show that compared with the L63T63 model, there are significant improvements in the simulated SST anomalies of LICOM during the El Niño period. In the L30T63 model, the warming caused by westerly wind anomaly is mainly located in the western side of the maximum wind stress anomaly, whereas in LICOM, the warming center is basically consistent with the position of the maximum wind stress anomaly, and the intensity of simulated SST anomaly enhances too. It is attributed to the fact that the maximum of simulated equatorial upwelling in the L30T63 model is roughly one second less than in LICOM, and its position in the former is much more eastward than in the latter. In the L30T63 model, warming is mainly caused by advection, whereas in LICOM, the westerly wind anomaly causes the equatorial upwelling to weaken. Therefore, in the high-resolution model, the variation of convection is the main reason for oceanic warming during El Niño, which is consistent with the observation and reflects the influence of the Kelvin wave.

Two sets of experiments are conducted. By using the assimilation data with or without the Argo data as the initial conditions, we utilize the global ocean-atmosphere coupled model to perform hindcast simulations in 1998-2003. The initial atmospheric conditions of the coupled model are obtained by interpolating NCEP reanalysis data at 00:00 and 12:00 on 11-14 May 1998-2003. The initial oceanic conditions employ the ocean assimilation of BCC-GODAS with or without the Argo data on 30 May 1998-2003. The coupled model is integrated to August 31 each time. The hindcast rainfall, air temperature, geopotential height, wind, and sea temperature in the summer (JJA) of 1998-2003 are calculated on the basis of the ensemble mean results.

The correlation coefficients between the hindcast and observation SST anomalies are shown in Fig.4. When Argo data are used, the grid number of positive correction within 30°N-30°S accounts for 72.32%, which is 3.15 percentage points larger than the grid number of positive correlation with the absence of Argo data (about 69.17%). In the tropics, the area where positive correlation reaches the 95% confidence level (correlation coefficient above 0.7) increases notably, especially in the tropical Indian Ocean and the eastern-central Pacific. Fig.4c shows the differences between Fig.4a and 4b. It can be seen that there are positive values (shown in shadow) in most areas, which account for 55.31%. Therefore, the tropical and sub-tropical SST hindcast by the atmosphere-ocean coupled model are improved significantly when Argo data are used.

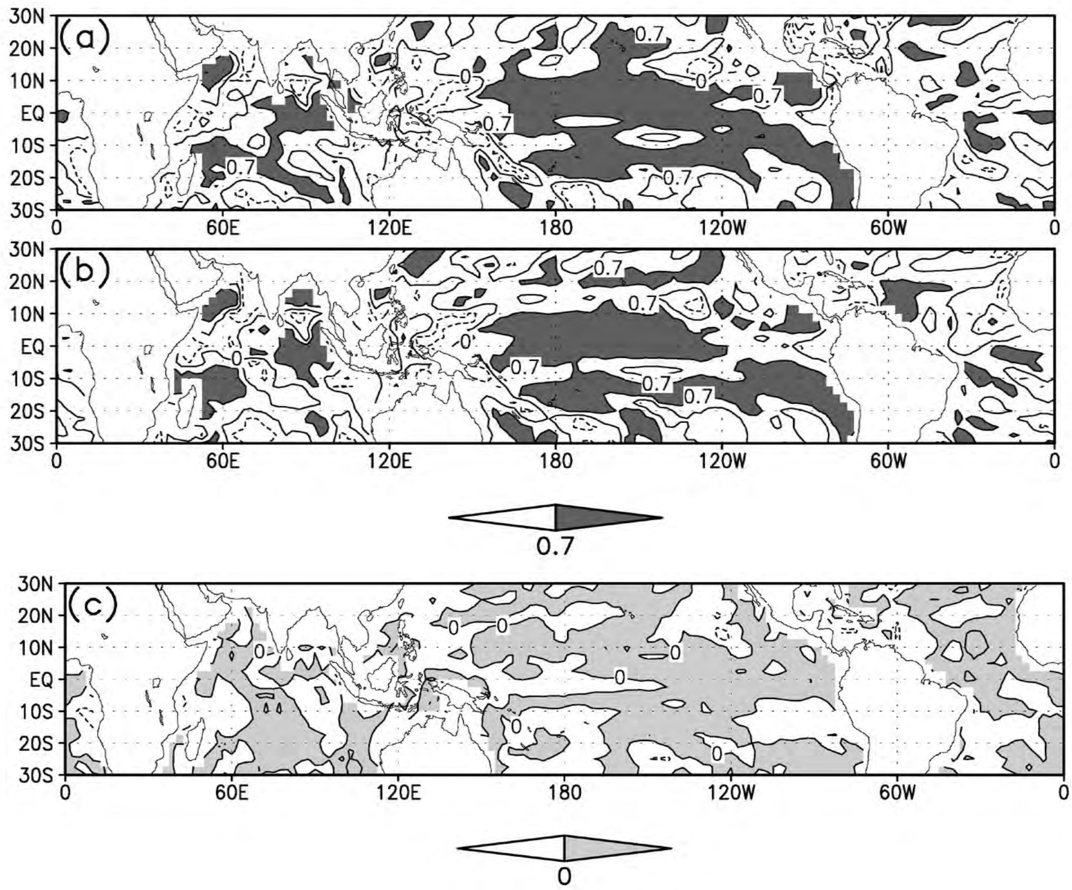

Figure 4. Correlation coefficients between hindcast and observation SST anomalies in the summers of 1998-2003. (a) Argo data used; (b) no Argo data used; (c) differences between (a) and (b). Light shadings indicate positive correlation, and dark higher than 95% confidence level.

Figure 5 shows the correlation between hindcasts and observations (Global Precipitation Climatology Project, GPCP) rainfall anomaly percentages. It is clear that the correlation coefficients in most areas of the globe are positive. When Argo data are used, the grid number of positive correlation accounts for 56.55%, which is 0.84 percentage point higher than the grid number of positive correlation (about 55.71%) when no Argo data are used (see Fig.5a and 5b). In the tropics, the area where positive correlation reaches 95% confidence level (correlation coefficient above 0.7) increases notably, especially in the tropical Pacific and Atlantic. Therefore, the accuracy of model hindcast for global precipitation increases slightly when Argo data are used. It can be seen from Fig.5c that the differences between the correlation coefficients with and without the use of Argo data are positive, which means that negative correlation coefficients decrease or become positive and thus the predictive skill is improved in most areas after Argo data are used.

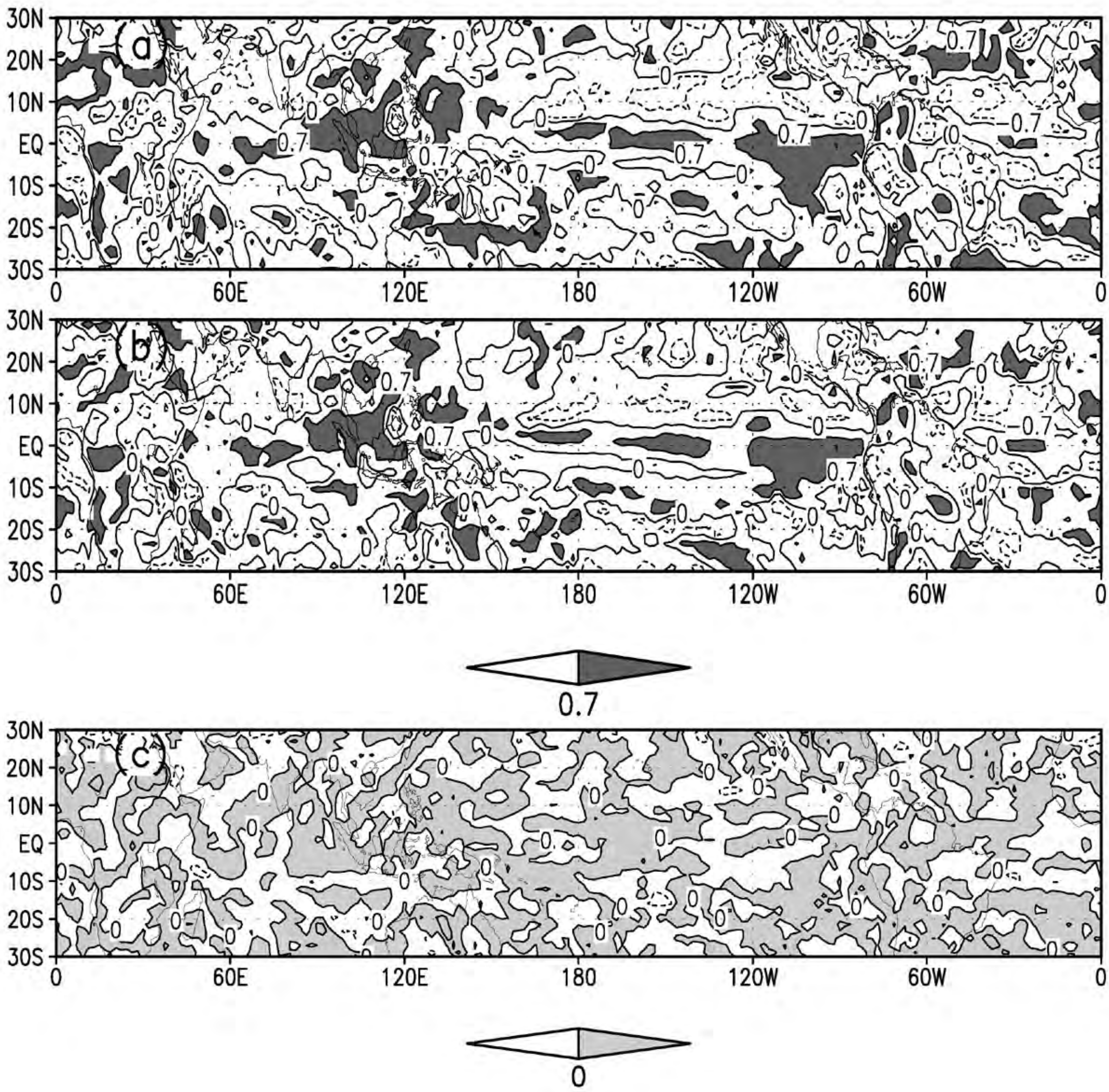

Figure 5. Correlation coefficients between hindcast and observation rainfall anomaly percentages in the summers of 1998-2003. (a) Argo data used; (b) no Argo data used; (c) differences between (a) and (b). Light shadings indicate positive correlation, and dark higher than 95% confidence level.

The correlation coefficients between the hindcast and observed rainfall anomaly percentages over China are shown in Fig.6. Comparing Fig.6a and Fig.6b, we can see that after Argo data are used, the area of positive correlation enlarges obviously. The originally negative correlation in North China, the regions between Yellow River and Huaihe River and between Yangtze River and Huaihe River, and that to the south of Yangtze River, and the eastern part of Xinjiang mostly change into positive correlation. When Argo data are used, the grid number of positive correlation accounts for 51.88%, which increases by 9.38 percentage points compared with that of positive correlation when Argo data are not used (about 42.5%, see Fig.6a and 6b). The differences between the correlation coefficients of rainfall anomaly percentages with and without Argo data are shown in Fig.6c. Further analyses indicate that the grid number of differences above zero accounts for 61.88%. Most regions of China are covered by positive correlation. It implies that compared with the situation without Argo data, positive correlation enlarges and negative correlation decreases or changes to be positive correlation in most regions of China when Argo data are used. Therefore, the accuracy of model hindcast summer rainfall over China increases significantly after Argo data are used.

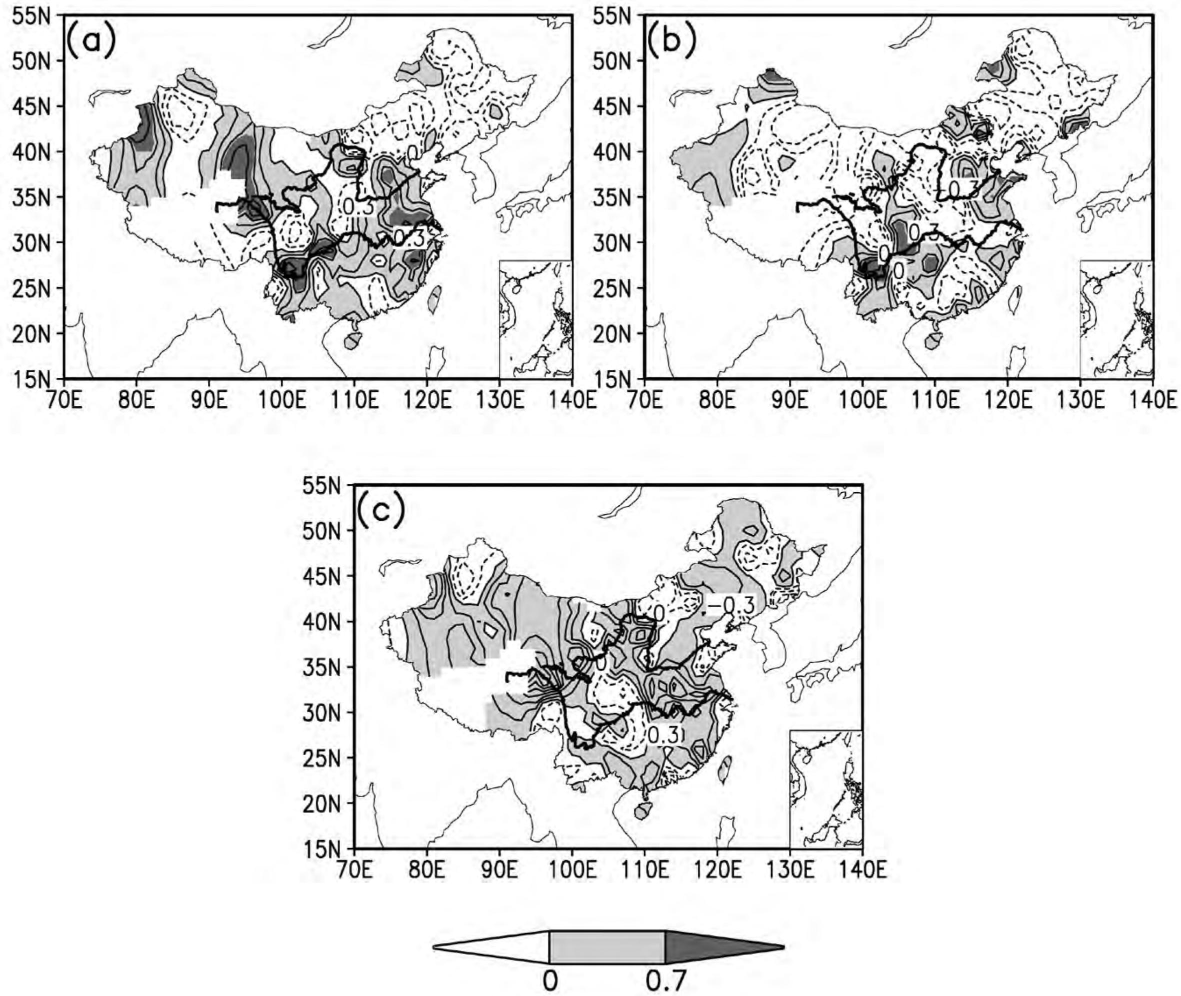

Figure 6. Correlation coefficients between hindcast and observation rainfall anomaly percentages over China in the summers of 1998-2003. (a) Argo data used; (b) no Argo data used; (c) differences between (a) and (b). Light shadings indicate positive correlation, and dark higher than 95% confidence level.

3.2 *Hindcast for 2002 summer case*

Ocean covers approximately 70% of the earth surface. It releases energy to the atmosphere in the form of sensible and latent heat and provides a large amount of water vapor to the atmosphere. Ocean plays a very important role in adjusting the atmospheric circulation and climate change. In order to analyze the effect of Argo data on the seasonal prediction of dynamical model in more detail, we take the summer (June, July, and August) of 2002 as example to study the summer rainfall anomalies over China.

In the summer of 2002, there was more than normal rainfall over the eastern part of the Northeast China, the Big Bend of Yellow River, the region to the south of Yangtze River, and the eastern and western part of Xinjiang. The rainfall over the most area of Northeast China, North China, the region between the Yellow River and Yangtze River and the central part of Xinjiang is less than normal (see Fig.7a). Fig.7b and 7c show the distribution of rainfall anomaly percentages over China in the summer of 2002 hindcast by AOGCM under the condition with or without Argo data. It can be seen from Fig.7 that, compared with the condition when no Argo data are used, the hindcast rainfall anomalies over China in the summer of 2002 are closer to the observation and the hindcast rainfalls improve obviously when the ocean assimilation data with Argo data are used as the initial field of AOGCM. For instance, the

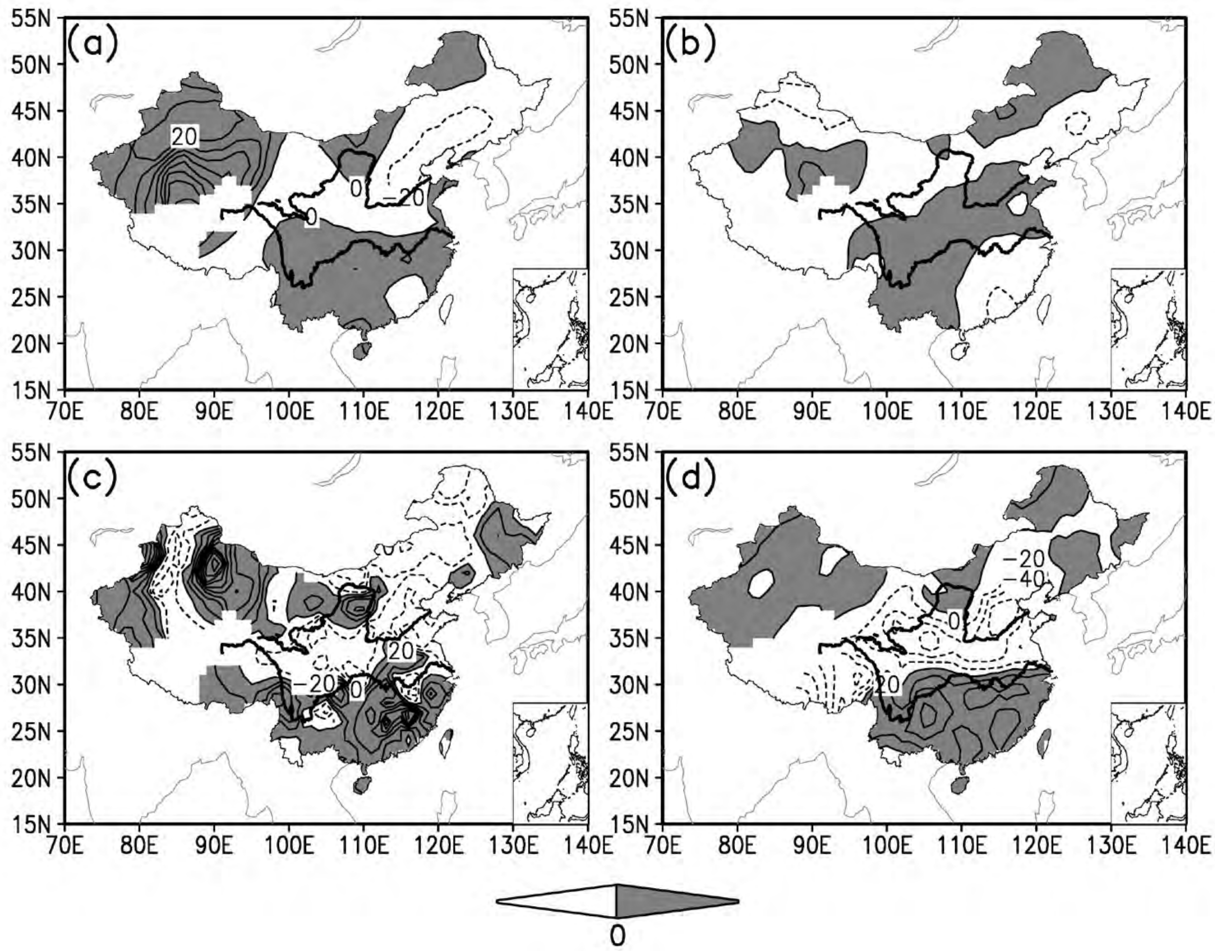

Figure 7. Hindcast (a, b) and observed (c) rainfall anomaly percentages, and the differences between hindcast rainfall amounts with Argo data and those without Argo data (d) over China in summer 2002. (a) hindcast with Argo data; (b) hindcast without Argo data; (c) observation; (d) differences between hindcast with Argo data and that without Argo data. Contour intervals of Fig.7a, b, and c are 20%. Contour interval of Fig.7d is 20 mm mon^{-1}. Positive values are shaded.

hindcast rainfall over the region between Yellow and Yangtze River changes from the originally more than normal (without Argo data) to less than normal (with Argo data), but the hindcast rainfall over the region to the south of Yangtze River turns from the originally less than normal to more than normal. The distinct changes of hindcast rainfall under the two conditions can also be found in Fig.7d. In other words, when Argo data are used, the rainfall over the region to the south of the Yangtze River increases notably, while the rainfall over the region to north of the Yangtze River decreases notably.

Figure 8 shows the differences of hindcast 500-hPa geopotential height, 850-hPa water vapor, and 850-hPa water vapor transport in the summer of 2002 under the circumstances with and without Argo data. It can be seen that a strong southerly air flow coming from the tropical region (such as the Bay of Bengal, western Pacific Ocean, and South China Sea) transfers water vapor to the region to the south of the Yangtze River in China, resulting in more than normal precipitation there (Zhang[26]). On the other hand, the Western Pacific Subtropical High (WPSH) is stronger than normal and controls the northern part of China. An anticyclonic and divergent air flow leads to less than normal rainfall over the region to the north of Yangtze River in China.

2002 is a weak El Niño year. In the summer, the tropical central and eastern Pacific SST was anomalously warmer than normal. There were weak warm anomalies over the Bay of Bengal and the tropical western Pacific Ocean (Figure not shown here). Because there are large differences between the climatological mean SST of assimilation and that of observation (see Fig.1c), the difference between the assimilated SST with Argo data and the observation is similar to the difference between the assimilated SST without Argo data and the observation (Figure not shown here). Fig.9a and 9b show the differences between the initial sea temperature fields of BCC-GODAS with and without Argo data on 30 April 2002. However, as shown in Fig.9a, the most significant improvement occurs in the simulation of SST in the Indian and North Atlantic Ocean after Argo data are used. For example, the unreal cold in the eastern part of Indian Ocean and the unreal warm in the western part of Indian Ocean decrease, and the illusive warm and cold in the North Atlantic diminish. The tropical Pacific SST between 20°N and 30°S has also been improved, with the deceasing of unreal warm or cold SST. However, there is no significant improvement in some regions of the middle and high latitudes of the Pacific (north of 20°N and south of 30°S).

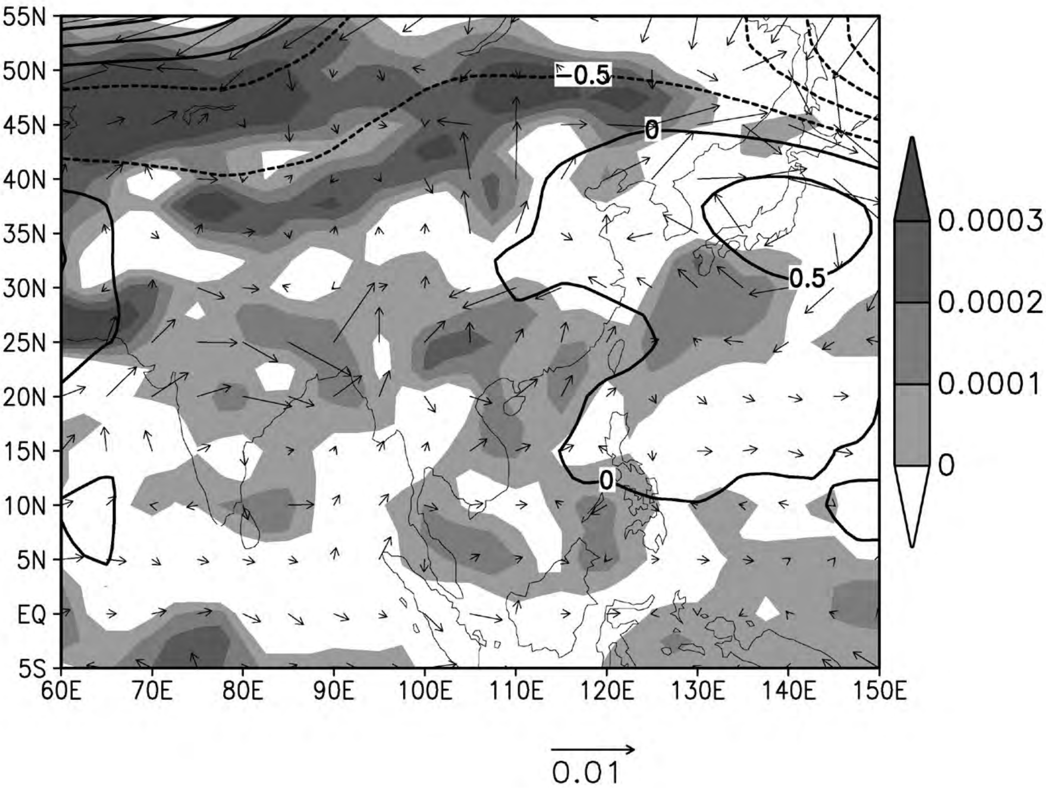

Figure 8. Differences of 500-hPa geopotential height (contour, unit: m), 850-hPa water vapor (shadings, unit: kg), and 850-hPa water vapor transport (vector, unit: kg kg^{-1} m s^{-1}) in summer 2002 between AOGCM hindcasts with and without Argo data.

It can be seen that when Argo data are used, the initial SST in the tropical western Pacific, tropical northern Pacific (10°N to EQ), tropical eastern Pacific (EQ to 30°S), eastern part of the Indian Ocean becomes warmer, with positive anomalies ranging from 0 to 0.8℃. In the Bay of the Bengal and the South China Sea, it is a little warmer ranging from 0 to 0.4℃.

In fact, between 20°N and 20°S in the tropical Pacific and Indian Oceans, the largest differences between the assimilated data with and without Argo data appear in the subsurface layer and upper layer ocean between 0 and 2 000 meters. The former is much warmer than the latter (see Fig.9b). The huge oceanic heat inertia makes the variation of the SST less than the variation of land surface temperature, which plays a buffering and adjusting role in the variation of atmospheric temperature. In the climate system, oceanic movement is a slow process as well as a source of major signals of prediction on the seasonal to interannual timescales. Because oceanic movement is a slow process, the vertical movement in the ocean (the upwelling and downwelling of sea water) causes deep-layer ocean to act on the upper-layer ocean continually and slowly, and influences the atmospheric circulation and water vapor transport through surface-layer ocean (such as SST anomalies), and finally influences the summer rainfall over China.

From Fig.9b, it can be seen that there are large differences between the assimilation results with and without Argo data in 100-2 000 meters in the Indian Ocean and 800-1 400 meters in the Pacific, probably due to the increase of Argo observation data. Most of the previous oceanic observation can only provide data in the upper 400-meter ocean, and the observation regions are mainly located in the Pacific. The Argo observation program provides much wider, denser, and deeper (up to 2 000 meters) oceanic observation data. Therefore, it is in favor of improving ocean data assimilation results.

Figure 10a shows the differences of precipitation in JJA 2002. Compared with the observation, the hindcast of global precipitation is generally more than the observation, with the largest difference being 800 mm mon^{-1} (Figure not shown here). It can be seen from Fig.10a that, after Argo data are used, the simulated precipitation in the polar and high latitudes decreases significantly, and the difference of precipitation decreases somewhat in some regions of China.

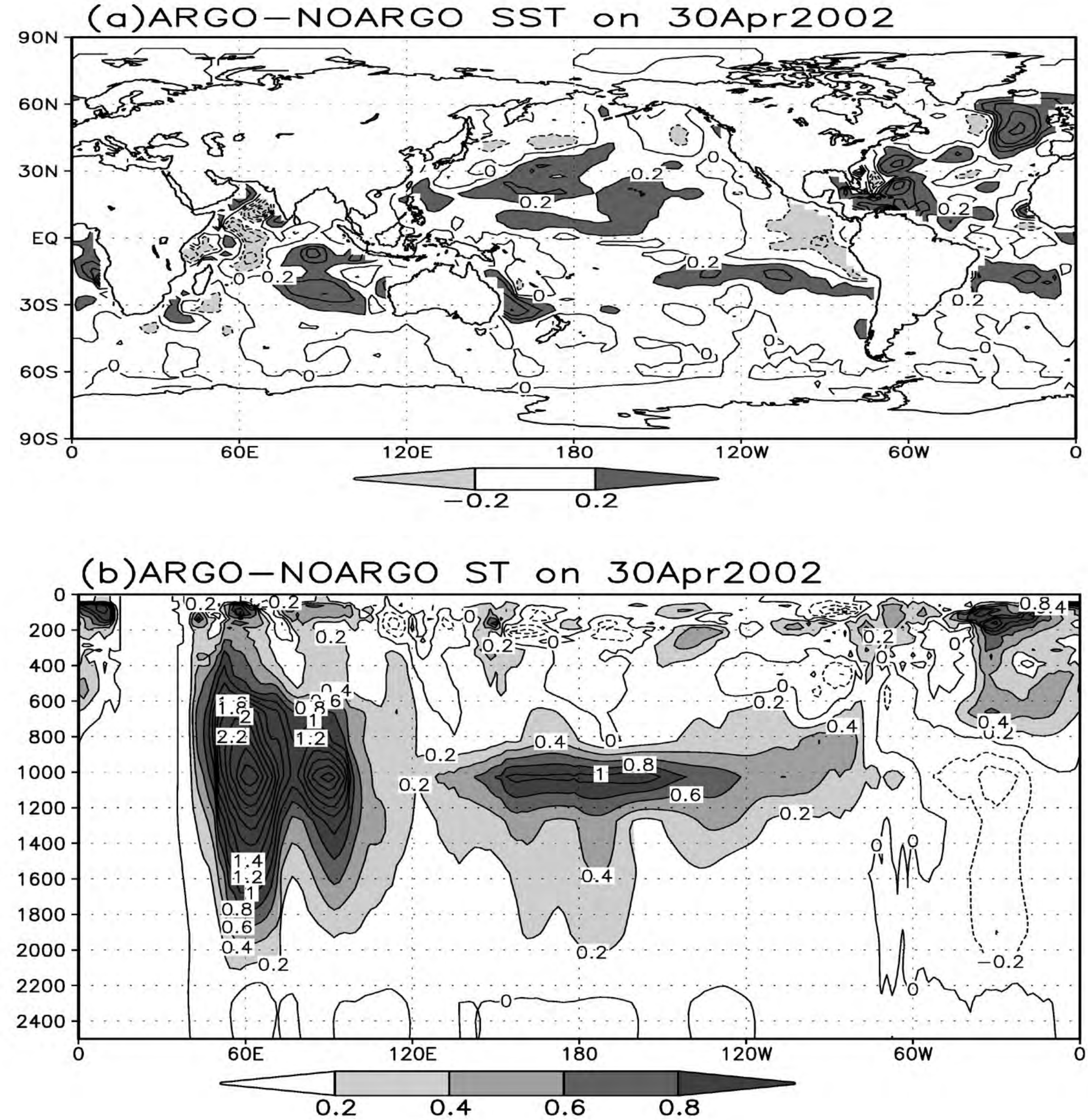

Figure 9. Differences of sea temperature on 30 April 2002 between BCC-GODAS assimilations with and without Argo data. (a) sea surface temperature; (b) longitude-depth cross section of sea temperature averaged along 20°N-20°S. Contour interval is 0.2℃.

Figure 10b shows the differences of SST in JJA 2002. The errors of hindcast SST in the tropical regions (30°S-30°N) range from 0 to 1℃. The error is large in the middle and high latitudes, with the maximum being around 4℃. After the Argo data are used, there is significant improvement of the hindcast SST in the Indian and Atlantic. For example, the cold SST bias in the middle and eastern part of the Indian Ocean and the warm SST bias in the western part of it decrease. Moreover, the SST errors in the Atlantic are also weakened.

4 CONCLUSIONS

In the present paper, the assimilation data from a global oceanic data assimilation system (BCC-GODAS) with Argo data are analyzed. The results indicated that the RMSE of the assimilated SST in most areas of the global ocean generally decreases, significantly in the North Atlantic and the Indian and Pacific Oceans. The application of Argo data in BCC-GODAS leads to notable improvement in assimilation effects. Compared with the observation data, the assimilated SST of BCC-GODAS can well describe the climatological state of SST. The grid number of positive correlation between the assimilated and observed SST anomalies accounts for 83.57% of the global ocean grids. Correlation between the assimilated and observed SST anomalies becomes better in the low latitude regions than in the middle and high latitude regions. The mean correlation coefficients in Niño3 and Niño3.4 regions of the tropical Pacific are 0.87 and 0.90, respectively. Both sea sur-

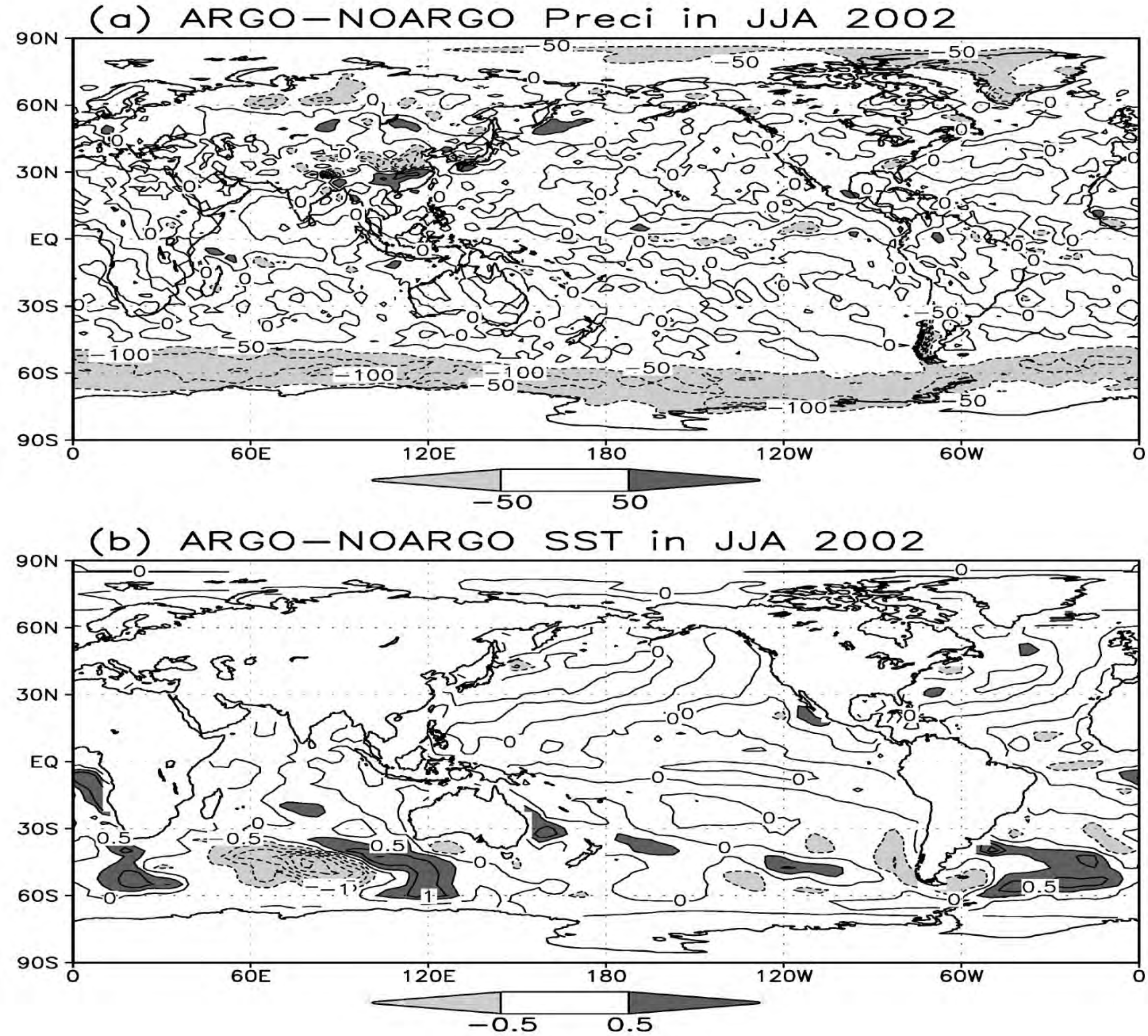

Figure 10. Differences of precipitation (a, unit: mm mon^{-1}) and sea surface temperature (b, unit: ℃) in summer 2002 between AOGCM hindcasts with and without Argo data.

face and subsurface temperature anomalies of BCC-GODAS have highly positive correlation with the NCEP_GODAS's assimilated data in the Pacific. Therefore, BCC-GODAS's assimilated SST and sub-surface temperature are consistent with the assimilated data from the assimilation system of NCEP_GODAS.

By using the two sets of ocean assimilation data with or without Argo data as the initial conditions respectively, a global atmospheric-oceanic coupled model is used to conduct hindcast experiments for the summer (June-July-August) of 1998-2003. The results show that when initial fields include Argo data, the tropical and sub-tropical SSTs hindcast by the coupled model have been obviously improved and the hindcast accuracy of global precipitation increases slightly. When Argo data are used, the area of positive correlation obviously enlarges, and the distribution pattern of hindcast summer rainfall over China is more consistent with the observation, and the hindcast accuracy increases significantly. When Argo data are used in the assimilation data, the grid number of positive correlation between the hindcast and observation SST anomalies between 30°N and 30°S (accounting for 72.32%) are 3.15 percentage points higher than the grid number of positive correlation when no Argo data are used (accounting for 69.17%). In China, when Argo data are used, the grid number of the positive correlation (accounting for 51.88%) is 9.38 percentage points higher than that when no Argo data are used (accounting for 42.5%). Therefore, when Argo data are used, the area of positive correlation obviously enlarges, and the distribution pattern of hindcast summer rainfall over China is more consistent with the observation, and the hindcast accuracy increases significantly. When the initial field comprises Argo data, the prediction effect can be significantly improved, and the ability of the global ocean-atmosphere coupled model increases in making seasonal prediction of the summer rainfall over China.

The detailed analyses for the case of summer 2002 show significant contrast when different initial conditions are used. By using the assimilation data with Argo data as initial condition, the summer rainfall anomalies over China in 2002 hindcast by the global ocean-atmosphere coupled model are much closer to the observation and the hindcast precipitation over the eastern part of China improves significantly. Analyses of the 500-hPa geopotential height, 850-hPa water vapor and the transport of water vapor show that in summer 2002, the southerly air flows from tropical regions (such as Bay of Bengal, western Pacific and South China sea) transport water vapor to the region to the south of Yangtze River in China and bring more rainfall there. Besides, the WPSH is stronger than normal. The northern part of China is under the control of high pressure, which causes less precipitation in the region to the north of Yangtze River in China. The ocean continually and slowly influences the atmospheric circulation and the transport of water vapor through the thermal state of the oceanic surface, and finally influences the summer rainfall over China.

Seasonal prediction of the global atmospheric-oceanic coupled model directly depends on initial and boundary condition. Improving the accuracy of initial and boundary field is important to the increase of predictive skill (Zheng et al.[5-8]; Yue et al.[26]; Zhang et al. [27-28]). The analysis results in this paper demonstrate that the assimilation results are improved greatly due to the introduction of Argo data into BCC-GODAS. The existing research (Zhang and Li[16]) shows that there are close relationship between the short-term climate variation in China and SST anomalies in some regions of the Pacific and Indian Oceans. The variability of the East Asian monsoon is greatly influenced by the SST anomalies in the tropical eastern Pacific, western Pacific Warm Pool and tropical Indian Ocean. It means that the dynamical short-term climate predictability in China should depend on the capability of a better description of the SST evolutions in these areas in the coupled model. Since Argo program provides much wider, denser, and deeper (up to 2 000 meters) oceanic observation data, the benefits of assimilating Argo in climate forecast are reflected not only from the surface (SST), but also from the improvements of upper oceans, such as ocean heat content, which is also indicated in Fig.9 of the present paper. The assimilation data comprising Argo information provide more substantial oceanic initial data for the ocean-atmosphere coupled model to perform short-term climate prediction, especially in China, which play an important role in the increase of seasonal prediction skill. At present, an oceanic data assimilation system with Argo data and an associated data bank have been established in BCC/CMA. The oceanic assimilation data comprising Argo data have been applied in the short-term climate operational prediction system of BCC/CMA.

REFERENCES:

[1] WCRP. CLIVAR Science Plan. [M]. WCRP Pub. No.89, WMO/TD-No.690, Geneva: World Meteorological Organization, 1995.

[2] LI Qing-quan, YANG Song, KOUSKY V E, et al. Features of cross-Pacific climate shown in the vari abilityof China and United States precipitation [J]. Int J Climatol, 2005, 25, 1 675-1 696.

[3] LI Qing-quan, SUN Cheng-hu, YUAN Yuan, et al. Major advances of China climate monitrong and diagnostic operation in recent 20 years[J]. J Appl Meteorol Soc, 2013, 24 (6) : 666-676 (in Chinese) .

[4] RONG Xin-yao, ZHANG Ren-he, LI Tim. Impacts of Atlantic sea surface temperature anomalies on Indo-East Asian summer monsoon-ENSO relationship [J]. Chin Sci Bull, 2010, 55(22): 2 458-2 468.

[5] ZHENG Fei, ZHU Jiang, ZHANG Rong-hua, et al. Improved ENSO forecasts by assimilating sea surface temperature observations into an intermediate coupled model [J]. Adv Atmos Sci, 2006, 23(4): 615-624.

[6] ZHENG F, ZHU J, ZHANG R H, et al. Ensemble hindcasts of SST anomalies in the tropical Pacific using an intermediate coupled model [J]. Geophys Res Lett, 2006, 33: L19604, doi:10.1029/2006GL026994.

[7] ZHENG F, ZHU J, ZHANG R H. The impact of altimetry data on ENSO ensemble initializations and predictions [J]. Geophys Res Lett, 2007, 34: L13611, doi: 10.1029/2007GL030451.

[8] ZHENG F, ZHU J. Coupled assimilation for an intermediated coupled ENSO prediction model [J]. Ocean Dyn, 2010, 60: 1 061-1 073, doi: 10.1007/s10236-010-0307-1.

[9] China Argo Real-time data Center. Advance in Implement of International Argo Program [J]. Argo Newsletter, 2006, 8: 21.

[10] XU Jian-ping. Argo global oceanic observation exploration [M]. Beijing: China Ocean Press, 2002: 115.

[11] XU Dong-feng, LIU Zeng-hong, XU Xiao-hua, et al. The influence of typhoon on sea surface salinity in the Warm Pool of the Northwest Pacific [J]. Acta Oceanol Sinica, 2005, 27(6): 1-7.

[12] LIU Zeng-hong, XU Jiang-ping, Zhu Bo-kang, et al. Upper ocean response to tropical cyclones in northwestern Pacific during 2001-2004 by Argo data [J]. J Trop Oceanogr, 2006, 25(1): 1-8.

[13] PAN Aai-jun, LIU Qin-yu. Mesoscale eddy effects on the wintertime vertical mixing in the formation region of the North Pacific subtropical mode water [J]. Chin Sci Bull, 2005, 50(1): 1-8.

[14] ZHANG Ren-He, LIU Yi-Min, YIN Yong-Hong, et al. Utilizing ARGO data to improve the ocean data assimilation and the relative physical processes in ZC ocean model [J]. Acta Meteorol Sinica, 2004, 6(5): 613-622.

[15] LIU Yi-min, ZHANG Ren-he, YIN Yong-hong, et al. The application of Argo data to the global ocean data assimilation operational system of NCC [J]. Acta Meteorol Sinica, 2005, 19(3): 355-365.

[16] ZHANG Ren-he, LI Qiang. Impact of Sea Temperature Variability of Tropical Oceans on East Asian Monsoon [J]. Chin J Meteorol, 2004, 30(12): 22-26.

[17] LIU Yi-min, LI Wei-jing, ZHANG Pei-qun. A global 4-dimensional ocean data assimilation system and the

studies on its results in the tropic Pacific [J]. Acta Oceanol Sinica, 2005, 27(1): 27-35.
[18] JIN Xiang-ze, ZHANG Xue-hong, ZHOU Tian-jun. Fundamental framework and experiments of the third Generation of IAP/LASG world ocean general circulation model [J]. Adv Atmos Sci, 1999, 16(2): 197-215.
[19] JIA Xiao-long, CHEN Li-juan, LUO Jing-jia. Climate prediction experiment for tropical cyclone genesis frequency using the large-scale circulation forecast by a coupled global model[J]. J Trop Meteorol, 2014, 20(2): 103-111.
[20] LI Yong-ping, LIANG Xu-dong, DENG Zhi-ying. Prediction of annual frequency of affecting tropical cyclone using the products of a hybrid coupled air-sea model [J]. J Trop Meteorol, 2001, 7(1): 63-68.
[21] LI Qing-quan, ZHAO Zong-ci. Diagnostic analysis and verification of prediction of the tropical Pacific sea surface temperature anomalies during 1997- 1998 [J]. J Trop Meteorol, 2001, 7(2):144-153.
[22] LI Qing-quan, DING Yi-hui, ZHANG Pei-qun. Primary verification and assessment on the extra-seasonally predictive capability of a global atmospheric-oceanic coupled model in raining season [J]. Acta Meteorol Sinica, 2004, 62(6): 740-751.
[23] YU Yong-qiang, ZHANG Xue-hong. Air-sea flux anomaly coupling scheme. Study on dynamical model for short-term climate prediction operation [M]. Beijing: China Meteorological Press, 2000, 201-207.
[24] YU Yong-qiang, ZHENG Wei-peng, ZHANG Xue-hong, et al. LASG coupled climate system model FGCM-1.0 [J]. Chin J Geophys, 2007, 50(6): 1 677-1 687.
[25] LIU Hai-long, ZHANG Xue-hong, LI Wei, et al. An eddy-permitting oceanic general circulation model and its preliminary evaluations [J]. Adv Atmos Sci, 2004, 21: 675-690.
[26] YUE Cai-jun, LU Wei-song, LI Qing-quan. The impact of initial forced wind on the predictability of the Zebiak-Cane coupled ocean-atmosphere model [J]. J Trop Meteorol, 2006, 12(1): 67-75.
[27] ZHANG Ren-he, YIN Yong-hong, LI Qing-quan, et al. Utilizing AGRO data to improve the prediction of ENSO and short-term climate prediction of summer rainfall in China [J]. J Appl Meteorol Sci, 2006, 17(5): 538-547.
[28] ZHANG Ren-he, ZHU Jiang, XU Jian-ping, et al. Argo global ocean data assimilation and its applications in short-term climate prediction and oceanic analysis [J]. Chin J Atmos Sci, 2013, 37(2): 411-424.

Citation: LI Qing-quan, ZHANG Ren-he and LIU Yi-min. Improvement of ocean data assimilation system and climate prediction by assimilating Argo data [J]. J Trop Meteorol, 2015, 21(2): 171-184.